The Iraqi Journal For Mechanical And Material Engineering, Vol.18, No2, June 2018

EXPERIMENTAL AND NUMERICAL STUDY OF NATURAL CONVECTION BETWEEN TILTED WALLS WITH ATTACHED FINS

Kadhum Audaa Jehhef **Mohamed Abed Al Abas Siba**
Email: kadhum.audaa@yahoo.com **Email:** Moh_siba@yahoo.com
[a]Ph.D., Department of Machines and Equipment, Institute of Technology,
Middle Technical University, Iraq

ABSTRACT
The free convection between two tilted adiabatic plates with centered heated horizontal cylinder with attached plate fin was investigated experimentally and numerically. The experimental rig constructed from vertical adiabatic was filled with air plates with aspect ratio of (A= 12) tilted by angles of (15^o, 30^o, 45^o, 60^o, 75^o, and 90^o). A horizontal heated cylinder with diameter of (16 cm) subjected under constant heat flux of (100, 500, 700, and 1000 W/m^2), the Rayleigh number ranging from (3.5×10^7 to 4.5×10^9). At the bottom of the rig left an opining with distance of (2, 4, 6, and 8 cm) but the upper left open to the atmosphere. The tested cases was of (without fin, smooth, triangular, square, and semi-circle fin) was attached to the right wall of the cavity. The numerical solution of the case was performed by solving the governing equations by ANSYS-FLUENT 14.0 package that dependent upon the finite volume method. The experimental results show that the Nusselt number increases with increasing Rayleigh number, decreasing the inclination angle, increasing heat flux and with increasing the bottom opining distance. Basically, the results showed that the using fins with any geometry will lead to increase the heat transfer rate. The optimum increasing in the Nusselt number was found by using triangular plat fin. Finally, the experimental data was compared with a numerical calculation and found that there is a good agreement in the same conditions.
KEYWORDS: Natural convection, parallel wall, heated cylinder, attached fins.

دراسة عملية ونظرية للحمل الحر بين جدارين مائلين بوجدود زعانف متصلة

د. كاظم عودة جحف **د. محمد عبد العباس سبع**
قسم المكائن والمعدات
معهد تكنولوجيا- بغداد، الجامعة التقنية الوسطى

الخلاصة

تم اجراء دراسة انتقال الحرارة بالحمل الحر عمليا وعدديا بين جدارين مائلين مع وجود اسطوانة مسخنة مركزية وتم تثبيت زعنفة صفيحية على احد الجدارين. يتضمن الجانب العملي في البحث الحالي تركيب جداران متوازيان مائلان بزوايا مختلفة مع الافق (15^o, 30^o, 45^o, 60^o, 75^o, 90^o) وبنسبة شكل ثابتة هي (A=12) والاسطوانة الافقية بقطر خارجي (16 cm) ومسخنة بواسطة فيض حرري ثابت هو (100, 500, 700, 1000 W/m^2) لقد تم استخدام عدد رالي بمقدار(3.5×10^7 to 4.5×10^9) اما اسفل الجدارين فقد تركت فتحة هوائية وبمسافات مختلفة هي (2, 4, 6, 8 cm) والجزء الاعلى من الجدارين فقد ترك مفتوحا للهواء الجوي. وقد تم دراسة اربع حالات تجريبية هي (بدون زعنفة، مع زعنفة ملساء، مع زعنفة مثلثة، مع زعنفة مربعة، مع زعنفة نصف دائرة) متصلة بالجدار الايمن للمغلف. اما الجانب العددي فتم تقديمه بواسطة حل المعادلات الحاكمة للحمل الحر بواسطة برنامج ANSYS-FLUENT 14.0

Received: 2017 -10 - 23
Accepted: 2018 - 1 - 28

المعتمد على طريقة الحجوم المحددة. وقد اظهرت النتائج العملية ان عدد نسلت يزداد مع كلا من زيادة عدد رالي ونقصان زاوية الامالة وزيادة الفيض الحراري وزيادة الفتحة السفلية للمغلف. اساسيا يمكن ملاحظة ان ادخال الزعنفة الى الحيز الداخلي للجدارين قد سبب زيادة في معدل انتقال الحرارة لكل التجارب، وان الزيادة المثلى في عدد نسلت وجدت عند استخدام الزعنفة المثلثية. واخيرا فان النتائج التجريبية قد قورنت مع النتائج العددية لقيم محددة وقد اعطت تطابقا ملموسا في توزيع درجات الحرارة.

الكلمات المفتاحية: الحمل الحر، جدران متوازية،اسطوانة مسخنة، زعانف متصلة.

Nomenclatures

A	aria of outer of cylinder surfaces, m^2.
Ar	cavity aspect ratio, Ar=H/W.
C, n	McAdams correlation constants.
d	diameter of the cylinder, m.
H	height of the two walls, m.
h_x	local convective heat transfer coefficient, $W/m^2.K$.
I	current, Amp.
L	length of the two walls, m.
m,n,*l*	number of grid points in x, y and z-directions.
Nu	Nusselt number, $Nu = hd/k$.
p	static pressure, pa.
Pr	Prandtl number, $Pr = v/\alpha$.
q"	surface heat flux, W/m^2.
Ra	Rayleigh number, $Ra = g\beta\Delta TW^3/\alpha v$.
Ri	Richardson number, $Ra = Gr/Re^2$.
s	opening distance, m.
t	iteration time, sec.
T	temperatures, K.
v	velocity vector component, m/s.
V	voltage, volt.
V	volume, m^3.
v_x,v_y,v_z	velocity in Cartesian coordinates.
W	gap distance, m.
x,y,z	Cartesian coordinates.
T_{amb}	air ambient temperature, K.
T_{av}	average thermocouple temperature, K.
T_w	cylinder surface temperature, K.
T_f	film air temperature, K.
cp	specific heat of the fluid, kj/kg.K.
g	gravitational constant, m/s^2.
k	thermal conductivity of the fluid, W/m.K.
k_{ref}	referenced thermal conductivity of the fluid, W/m.K.
G_k	represents the generation of turbulence kinetic energy due to the mean velocity gradients.
G_b	generation of turbulence kinetic energy due to buoyancy.
Y_M	represents the contribution of the fluctuating dilatation.
k	turbulence kinetic energy, m/sec^3

Greek Letters

α	fluid thermal diffusivity, m^2/sec**.**
β	fluid compressibility, K^{-1}.

μ fluid dynamic viscosity, Pa.sec.
ν fluid kinematic viscosity, m^2/sec.
ρ density of the air, kg/m^3.
θ inclination angle, degree.
ϵ rate of dissipation, m_2/sec^3
σ_k, σ_ϵ turbulent Prandtl numbers for k and ε.
ξ computed field variables.

INTRODUCTION

Convective heat transfer is a phenomenon of practical and functional importance with wide range of scientific and engineering applications. The heat transfer classical theory was written to investigate the heat transformation between hot substance and its environment. The heat transfer by natural mode refers to the movement of the fluid via the buoyant forces arising caused by the gradients of the fluid density due to the gradients of the temperature Simon, et al. [2015]. Natural convection in enclosures has been studied extensively over the past years Roslan, et al. [2014], and Fariborz, et al. [2016]. The effect of attached fins on the natural convection heat transfer rate was presented in number of studies as followed. The free convection from fins attached to the heated wall inside inclined rectangular enclosures presented by Lakhal, et al. [1997] at Rayleigh number 10^2>Ra>2×10^5, the aspect ratio given by ($2.5\leq A=H'/L'\leq 8.5$) and the tilted angle in the range of $0\leq\theta\leq60^o$. They showed that the presence of the fins will considerably effect on heat transfer through. Also, Ahmed and Sakr [2005] presented a numerical study in the effect of conducting fins attached to the hot vertical wall on the free convection heat transfer in vertical cavities. They observed that the heat transfer rate through an enclosure was affected greatly by the number of the attached fins. Bilgen [2005] gave a numerical study in differentially heated square cavities with Rayleigh number from 10^4 to 10^9 and dimensionless thin fin length from 0.10 to 0.90. He was found that Nusselt number is an increasing function of Rayleigh number, and a decreasing function of fin length. A thin fin was attached on the active wall. It was found that Nusselt number is an increasing function of fin length. However, Ahmed [2006] studied the laminar natural convection in vertical enclosures with conducting fins attached to the hot vertical wall. He showed that the fins affected on the heat transfer rate and it can be controlled by the number of the attached fins. Also, Abdullatif and Ali [2007] presented a numerical study in the free convection from inclined thin fin of arbitrary length in a square enclosure. Moreover, an experimental study of the natural convection in horizontal and vertical narrow enclosures with heated rectangular finned base plate presented Nada [2007]. The results showed that at maximum Nusselt number (Nu) and finned surface effectiveness (e), the fin spacing will be in an optimum. Olivier, et al. [2008] studied the natural convection from a single and two horizontal cylinder cases for Rayleigh numbers of 2×10^6, 4×10^6 and 6×10^6. They showed that the heated cylinders give a plume that rising from the heated lower cylinder until to attach the above cylinder. However, Jani, et al. [2012] gave a numerical investigation on the effect of fin attached to the cold wall on the free convection in differentially heated rectangular cavities. Their results were presented for a range of *Ra* from 10^3 to 10^6 with a fin at different lengths, *L* = 0.25, 0.5, and 0.75 and the aspect ratio of cavity which varies from 4 to 0.25. They showed that the effect of fin at low Prandtl numbers on enhancement of the heat transfer was more than that in high Prandtl numbers. Petr and Dvorak [2013] presented a study in natural convection flow around a horizontal cylinder in a space limited by rectangular cavity using four different diameters of horizontal cylinders. They noted that the results within the laminar range for Ra <10^8 have been obtained for the space limited by rectangular cavity with width corresponding two cylinder diameters. This limitation of space around horizontal cylinder has

a significant influence on fluid flow. Rahman, et al. [2014] developed an unsteady free convection model for heat transfer and fluid flow in a cavity with a middle hollow cylinder and they was applied three values of Grashof number are 10^4, 10^5 and 10^6. They showed that when the cooler was located at the middle of the vertical wall. Finally, Renato, et al. [2016] gave a theoretical investigation on the free convection from two inner bodies two inner bodies located inside a square enclosure for Grashof number was considered in range from 2×10^4 to 10^5. They were noted that the increasing the Grashof number will lead to increase the average Nusselt number. And the increasing in Grashof number results in higher velocities in fluid flow and more efficient heat exchange between fluid and cavity surface.

The main purpose of this work is to study the effect of plate aluminum fin geometry includes (smooth fin, equilateral triangular fins, rectangular fins and semi-circle). These fins were attached to the right wall of the two parallel vertical tilted walls on the convective heat transport from horizontal heated cylinder. This cylinder putted in the middle of the gap between the two walls these walls was inclined with tilted angle of (15^o, 30^o, 45^o, 60^o, 75^o, 90^o), but the top and bottom wall was opened to the atmosphere. The experiments was carried out under the following conditions; the Rayleigh number ranging by (3.5×10^7 to 4.5×10^9), the enclosure aspect ratio was fixed at (Ar=H/W=12) and inclination angle $0 \leq \theta \leq 60^o$

EXPERIMENTAL APPARATUS SETUP

A simple natural convection apparatus was given in a photograph in (**Figure 1**) and as schematic as shown in (**Figure 2)**. The present experimental rig was employed in this study consists of:

1. An air gap between two surfaces with dimensions (60 cm high, 40 cm long and 5 cm wide) was adapted for this study.
2. The right wall consists of asbestos plate with dimension of (40×60 cm) with thickness of (1.5 cm) and paper with thickness of (1 mm) and sheet of aluminum of thickness of (0.85 mm) in front of the test section.
3. A plate aluminum fin geometries include (smooth fin with length of 1.5 cm, equilateral triangular fins with height of 1.5 cm, rectangular fins with dimension of 1.5×1.0 cm and semi-circle of radius of 1.5 cm) attached to the right wall (**Figures 3 and 4)**.
4. The left wall consists of glass sheet with thickness of (6 mm).
5. The bottom side equipped with an opening with four cases of (2, 4, 6, 8 cm) which was opened to atmosphere.
6. The top side was opened to the atmosphere.
7. In the middle distance between the two walls there was a cylindrical heater element can be mounted horizontally in the air gap was heated by a heater of power of (1000W) cartridge heater. The heater inserted in a central bore with 10 mm diameter. The heater covered by a copper tube with outer diameter of (16 mm) and thinness of 1.0 mm it placed below the fin plate by a distance of (32 cm). The heated middle cylinder considered approximately at boundary condition of constant wall temperature during testing because the high thermal conductivity and low thickness of the copper cylinder metal.
8. The heater power controlled its supplied power voltage by using a variable voltage (variac) of (8 Amp) to perform a constant heat flux varies by (100, 500, 700 and 1000 W/m^2).
9. The right and lift walls and the air gap temperatures was recorded by using a (Type-T) thermocouples (6 in numbers) as shown in (**Figure 2)** and located equidistance to embark average air temperature. Also, the wall temperatures of the heater wall were recorded by three thermocouples. These thermocouples connected to the Lap. Jack U6 data question

and then collected by a PC computer. For the range of measurements presented the surface temperature has been observed to vary by less than 0.1 ^{o}C circumferentially.

Data Reduction

The local heat transfer by free convection in the experimental work can expressed by local heat transfer coefficient where it determined from the electrical power supplied that heat power lost due to the convection was found by Simon, et al. [2015].

$$h_x A \Delta T = VI \quad (1)$$

$$h_x = \frac{VI}{A \Delta T} \quad (2)$$

Where

$$\Delta T = (T_{av} - T_w) \quad (3)$$

Where (T_{av}) represent the average air temperature in the gap and given by:

$$T_{av} = \frac{T_1 + T_2 + T_3 + T_4 + T_5 + T_6}{6}$$

and the local experimental Nusselt number calculated from:

$$Nu_x = \frac{h_x d}{k} \quad (4)$$

The air film properties may be found at film temperature given by:

$$T_f = \frac{(T_{av} - T_w)}{2} \quad (5)$$

The average Nu found by:

$$Nu_{ave} = \frac{1}{W} \int_0^W Nu_x dy \quad (6)$$

The work primarily focuses on the implications of secondary heat transfer owing to external heat sink on transfer of natural convective heat transfer from the square plate.

Temperature Measurements Calibration

Thermocouples were tested from 100°C down to 0°C with the use of boiling water filled in a beaker of (5 liters) and a cooler of ice water. All (Type-T) thermocouples probes exhibited a slight offset from the actual temperature measured by the thermometer. In order to correct this offset a calibration equation was determined. Also, these thermocouples (6 in numbers) and the (Lap.Jack U6) data question calibrated before using according to (Central Organization for Standardizations and Quality Control, Baghdad, Iraq) standardization with a maximum error of about (±0.12 ^{o}C).

Error Analysis

When attempting to correlate or compare experimental results with numerical simulations, it is imperative that the issues of errors and uncertainties are addressed. In this section, the various sources for errors and uncertainties in the experimental for this work are identified. The experimental errors were introduced during the experimental investigation such as (Measurement uncertainties…etc.) in-depth analysis and discussion of the errors involved by Holman [2012]. The results of this analysis may be summarized by (Table 1).

NUMERICAL SOLUTION

Geometry Construction

The flow regime induced by buoyancy about a confined, heated horizontal cylinder inside two parallel inclined walls, a three-dimensional model was created and computed a CFD flow modeling simulation software program by ANSYS FLUENT 14.0. The problem domain geometry and the boundary conditions presented in **(Fig.5)**.

Equations of Flow

The buoyancy-induced problems formulation solved according the basic conservation principles that description the fluid movement, these equations named the conservation of mass, momentum, and energy, it can be presented via **ANSYS FLUENT 14.0 [2009]**:

$$\frac{d\rho}{dt} + \nabla.(\rho\vec{v}) = 0 \quad (7)$$

$$\frac{d}{dt}(\rho.\vec{v}) + \nabla.(\rho\vec{v}\vec{v}) = -\nabla P + \nabla.\vec{\tau} + \rho\vec{g} \quad (8)$$

The stress tensor of the momentum expression, $\vec{\tau}$, can be found by **Pletcher, et al. [2012]**:

$$\vec{\tau} = \mu\left[(\nabla\vec{v} + \nabla\vec{v}^T) - \frac{2}{3}\nabla\vec{v}I\right] \quad (9)$$

expansions and simplifications, Equations (8) and (9) can be rewritten as **Pletcher, et al. [2012]**:

$$\nabla.(\rho\vec{v}) = 0 \quad (10)$$

$$\nabla.(\rho\vec{v}\vec{v}) = -\nabla P + \mu(\nabla^2.\vec{v}) + \rho\vec{g} \quad (11)$$

The Oberbeck-Boussinesq approximation can be used in order to simplify the evaluation of the fluid density, and to linearize the density temperature dependency according the buoyancy force, thus the buoyancy force is represented by **Kuehn and Goldstein [1980]**:

$$\rho\vec{g} = \vec{g}\left[\rho_{ref} - \rho_{ref}\beta(T - T_f)\right] = \rho_{ref}\vec{g}\left[1 - \beta(T - T_f)\right] \quad (12)$$

where β is the fluid compressibility found by **Kuehn and Goldstein [1980]**:

$$\beta = -\frac{1}{V}\frac{\partial V}{\partial P} \quad (13)$$

Additionally, since at nominal atmospheric pressures and temperatures can expressed the air behaves as an ideal gas, the air compressibility can be expressed by **Kuehn and Goldstein [1980]**:

$$\beta = \frac{1}{T_f} \quad (14)$$

By simplifications equations (11) and (12) the final forms can be obtained by **Pletcher, et al. [2012]**:

$$\nabla(\vec{v}) = 0 \quad (15)$$

$$\vec{v}.(\nabla.\vec{v}) = -\frac{1}{\rho_{ref}}\nabla P + v_{ref}(\nabla^2.\vec{v}) + \vec{g}\left[1 - \beta(T - T_f)\right] \quad (16)$$

The standard k-ε model in ANSYS FLUENT falls within this class of models and has become the workhorse of practical engineering flow calculations in the time since it was proposed by **Launder and Spalding [1972]**. The general modified form of (k-ε) model can be written as follows:

$$\frac{d}{dt}(\rho k) + \nabla.(\rho k\vec{v}) = \nabla.\left[\left(\mu + \frac{\mu_t}{\sigma_k}\right)\nabla.(k)\right] + G_k + G_b - \rho\varepsilon - Y_M + S_k \quad (17)$$

and

$$\frac{d}{dt}(\rho\epsilon) + \nabla.(\rho\epsilon\vec{v}) = \nabla.\left[\left(\mu + \frac{\mu_t}{\sigma_\varepsilon}\right)\nabla.(\epsilon)\right] + C_{1\epsilon}\frac{\epsilon}{k}(G_k + C_{3\epsilon}G_b) - C_{2\varepsilon}\rho\frac{\epsilon^2}{k} + S_\epsilon \quad (18)$$

The turbulent (or eddy) viscosity, μ_t, is computed by combining k and ϵ as follows:

$$\mu_t = \rho C_\mu \frac{k^2}{\epsilon} \quad (19)$$

The model constants $C_{1\varepsilon}$=1.44, $C_{2\varepsilon}$=1.92, $C_{3\varepsilon}$=1.01, C_μ=0.09, σ_k=1.0, and σ_ε=1.3 have the following default values **Launder and Spalding [1972]**:

Boundary and Initial Conditions

Cylinder Surface wall: this boundary can be expressed by:

$$v_x = v_y = v_z = 0$$

a Neumann boundary condition can be used along the cylinder for heat flux is assumed to be constant as followed:

$$\frac{\partial T}{\partial n} = \frac{q''}{k_{ref}}$$

where n represent the direction normal to the surface.

Vertical Walls: the adiabatic boundary can be applied to the confining wall such as:

$$\frac{\partial T}{\partial n} = 0$$

Air Inlet / Outlet: These boundary conditions of the opening vent set as zero pressure expressed by:

$$\frac{\partial P}{\partial n} = 0$$

In this numerical study the following initial conditions were employed:

$$v_x(0,x,y,z) = v_y(0,x,y,z) = v_z(0,x,y,z) = 0$$

$$T(0,x,y,z) = T_{amb}$$

Grid Generation and Numerical Solution

The heat transfer studied parameters at heated horizontal cylinder surface for various heat flux fixed in the middle of two tilted plates was determine in this study, by using the finite-volume grids it was generated along whole geometrical domain. The Auto CAD and Gambit 2.3.16 software used to simplify the construction of each of this geometry and mesh files. Also, the tetrahedral mesh was employed in order to model the air space by 2017421 nodes or (20×120×80) in the x, y and z directions. A section of the mesh of cavity was presented in **(Figure6).** The three-dimensional mesh of the computational domain was exported to the ANSYS FLUENT 14.0 program. In this program to couple the inlet and outlet pressure boundary conditions the SIMPLE algorithm was employed. The model is terminated when the mass, momentum, and energy for each simulation evaluated over the course, residuals drop below 10^{-7}. Also, the pressure and momentum calculations were altered the under-relaxation factors at 0.70 and 0.30 respectively to improve the convergence rate of the models, but the density and energy were left at the default values. Moreover, in these numerical simulations, the convergence criterion for temperature, pressure, and velocity is Davis [1983]:

$$Error = \frac{\sum_{k=1}^{l}\sum_{i=1}^{m}\sum_{j=1}^{n}|\xi_{i,j,k}^{t+1} - \xi_{i,j,k}^{t}|}{\sum_{k=1}^{l}\sum_{i=1}^{m}\sum_{j=1}^{n}|\xi_{i,j,k}^{t+1}|} \leq 10^{-7} \quad (20)$$

Grid Independence Test

A grid independence test was performed to evaluate the effects of grid sizes on the results. Four sets of mesh were generated using tetrahedral three dimensional meshes with 85621 nodes, 129776 nodes, 1028433 nodes and 2017421 nodes. It was observed that the 2017421 nodes and 1028433 nodes produce almost identical results with a percentage error of 0.135%. Hence, a domain with 2017421 nodes was chosen to increase the computational accuracy. The summary of the grid independence test results is shown in (Table 2).

RESULTS AND DISCUSSION

The present work was carried out to investigate the effects of the following parameters: fin geometry, Rayleigh number and two walls orientation and bottom opening distance on the free convection heat transfer coefficients from heated cylinder between two walls filled with air between them has been investigated experimentally and numerically. The experiments were carried out by varying the power supplied to the cylindrical heater for four values of (100, 500, 700, 1000 W/m^2) and varying the opening of the bottom distance in the range of (2, 4, 6, 8 cm), and adjusting the title angle of the two walls by (15^o, 30^o, 45^o, 60^o, 75^o, 90^o) and

the Rayleigh number ranging from (3.5×10^7 to 4.5×10^9). The present experimental results of the partitions angle of 90^o were compared with the previous works such as Raithby and Wong (1981) at Rayleigh number range of (1.5×10^5 to 2×10^8) and Esherbiny, et al., (1982) at Rayleigh number range (2×10^5 to 8×10^8) presented in (Figure7) for the case of without fin of air across vertical air layers.

Experimental Results

To study the effect of increasing the heat flux of the cylinder from 3.5×10^7 to 8.4×10^8 the results of the temperatures distribution presented in **(Figures 8 a and b)**.at constant angles and opening length. The results show that the increased in the heat flux will increase the maximum temperatures in the center between the two walls, due to heat induced by buoyancy force of the fluid. In the other side the **(Figures 8 c and d)** presented the effect of decreasing the tilted angle from 90 to 60 will affect to change the profile the whole temperatures along the air gap and increased along the right wall. But, when increasing the bottom opening from 2 to 4 cm, show that the temperatures will decrease as show in **Figures 8 e and f** due to increasing the cooling rate of the air **in the gap.** The above results is for smooth plate fin attached on the right wall, while the temperature distribution in the air gap for the cases of using triangular, semi-circle and square plate fins plotted in the **(Figures 9, 10 and 11).** At any Rayleigh number and for all fin-models, the results showed that, the vertical and tilted enclosure temperatures variations with heated cylinder are lower than those of the case without fins. Especially in the case of triangular plate fin due to the increased of the air flow across the air gap and this lead to increase the heat transfer rate.

To summary the effect of plate fin models on the air Nusselt number (Nu) using **(Figures 12, 13 and 14)** for without fin and triangular fin only when increasing the heat flux and opening distance. The results show that for the two cases the Nusselt number increased with increasing the heat flux and opening distance and gives a same profile. The Nusselt number reaches a maximum at a gap center for the case of without fin but it rose along the left wall for triangular fin because the heated air currents pushed toward the left wall (no fin attached). But can be show that the triangular gives an increasing in the Nusselt number (Nu) as compared with the using without once for same conditions. In order to indicate the enhancement of using plate fin attached on the right wall of the enclosure focused on the **(Figure15)**, it will plot the experimental temperatures distribution along the air gap distance. The figure shows that the using triangular fin will increase the temperatures as compared with the other fin models due to increase the air flow across the air gap especially in the region above the plate fin. **(Figure 16)** presented a comparison between the four fin plate models employed in this study with the case of without fin in the variation of Nusselt number (Nu) variation along the distance between two vertical walls. The results show that the triangular fin plate by 66% and 54% 50%, 36% for using triangular, circle, square and smooth respectively. The experimental results of the average Nusselt number (Nu) with average Rayleigh number (3.5×10^7 to 4.5×10^9) was plotted **(Figure 17).** The results showed that the (Nu) increased with Rayleigh number for all fin models tested in this study with different present of error. According to experimental data available, there is an acceptable fit provided that $10^3 < Ra < 10^9$ for **Gebhart, et al. [1988**] and **McAdams [1954]** correlation**. Morgan [1975**] expanded on McAdams work to present an expression of:

$$Nu = CRa^n \quad (21)$$

The obtained parameter from the present experimental study for all employed cases presented in (**Table 3**) for range of Ra between (3.5×10^7 to 4.5×10^9).

4.2 Numerical Results

The numerical solution by computational fluid dynamics ANSYS FLUENT 14.0 program is employed to investigate the natural convection fluid flow and heat transfer between two vertical walls with a fin attached to right wall. The results are presented for a range of Rayleigh number of 10^8 for without fin, with smooth fin and with triangular fin at constant length, (L = 1.5 cm), the Prandtl number is (Pr=1.17) the aspect ratio of cavity which constant at (A=12). **(Figures 18 and 19**) show the streamlines and the isotherms for without and with smooth fin models. The fluid that is heated by heated horizontal cylinder that rises toward the attached plate fin and recirculating near the upper surface of the fin. The presence of the fins will cause to increase the momentum of the fluid in the zone upper the heated cylinder thus will increase the natural convection heat transfer by turbulent the heated air and replaces the cooled fluid next to the right wall by the rotating vortex (also called the primary vortex). For a larger Rayleigh number (Ra= 10^8), the temperatures and velocity distribution is fairly uniform in the case of the without fins and is slightly disturbance and non-uniform than the case of with smooth fin attached. Between $30° < \theta < 90°$, as the flow moves tangentially around the heated cylinder the boundary layer thickens will increase. At $\theta = 30°$, the temperature rises significantly, and we will observe a flow separation from the cylinder surface and there is a plume formation and when using a smooth fin show an increasing the temperatures distribution behind the fin. The profile of radial velocity and temperatures distributions normal to the surface of the air gap for two angles of $\theta=30^o$ and 90^o in three regions of the fin plate location used to expressed the nature of the flow of free convection was plotted in **(Figure 20)**. The decreasing the orientation angle from 90^o to 30^o will effect on the temperature profile by raised it towered the left wall. Also, the velocity will affect by changing the walls tilted and make the profile more fluctuating than the vertical angle. But decreasing the angle will decrease the maximum velocity of the hot air that flows in the gap due to decreasing the buoyancy force of the hot air. The results show that the using smooth fin attached to the wall plotted in **(Figure 21)** will lead to change the profile of the temperatures of the two angles. The study of the effect of all orientation angles from 30^o to 90^o wal plotted in the **(Figure 23)** at q"=500 W/m^2, s=4 for case of without plate fin. The numerical results show that in the vertical position the temperature profle was uniform along the air gap. Finally, the comparison between the experimental and numerical results was presented by using the results of two walls of the without fins at $\theta=90^o$, (Ra=4.5×10^8), t=10 min, s=4 cm. the figure shows good agreement between the two results at the same conditions.

CONCLUSIONS

The heat transfer by natural convection in inclined two adiabatic parallel plates at aspect ratio of (A=12) with four models of aluminum fins of (smooth, triangular, semi-circle and square) attached to the right wall with horizontal centered heated cylinder subjected to constant heat flux has been studied numerically for Ra (3.5×10^7 to 4.5×10^9). The present experimental work showed that:

- The average (Nu) of the cavity increases with increasing the (Ra) for all the cases
- The average Nusselt number increases monotonically with increasing the inclination angle (θ), with increasing heat flux (q") and with increasing the bottom opining distance (s).
- Also, the results found that the using attached fins on the right wall of the cavity with any fin geometries will lead to increases the coefficients of the natural convection heat transfer due to increasing the turbulence of the air flow and then increasing the Nusselt number.
- Finally, the optimum increasing in the Nusselt number was found by using triangular fin.

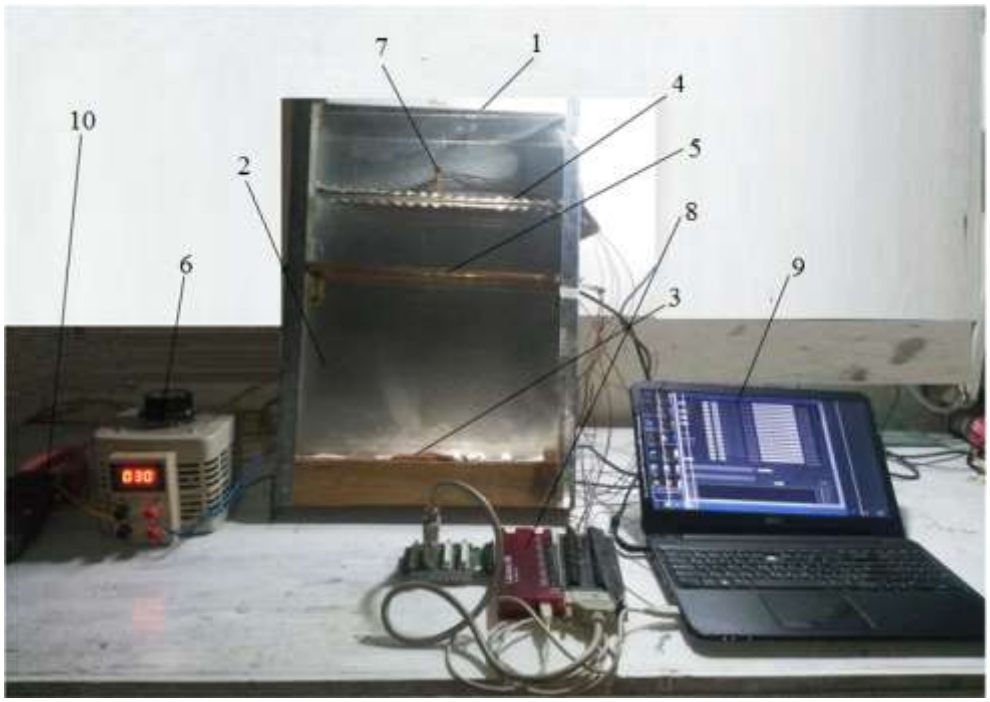

Fig.1: Pictorial view of the experimental apparatus setup includes: 1) Insulated plate, 2) Front glass wall, 3) Air opening, 4) Plate fins, 5) Heater source, 6) Voltage variable, 7)Thermocouples, 8) Data equistion, 9) PC computer and 10) Millimeter.

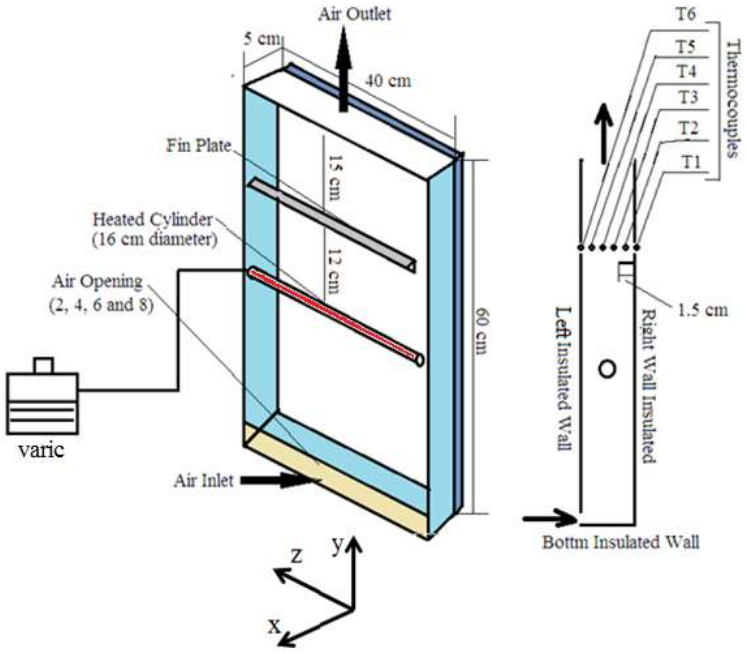

Fig.2: Schematic of the experimental apparatus.

Fig.3: Pictorial view of the tested plate fins.

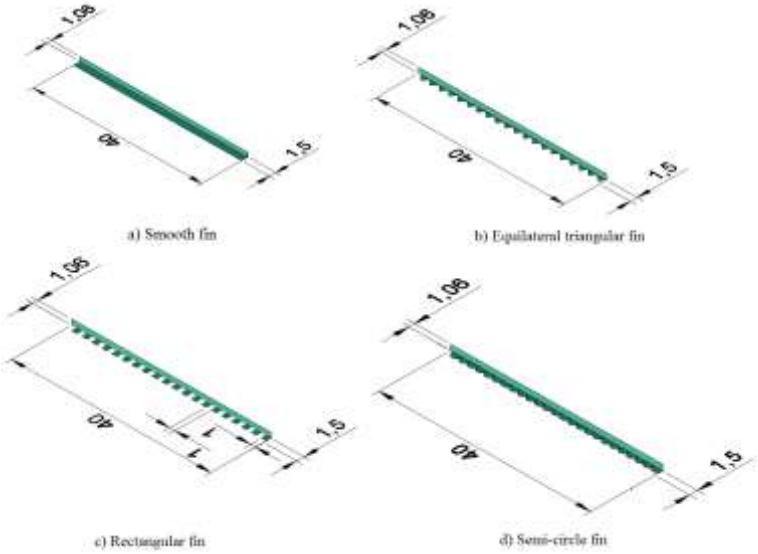

Fig.4: Pictorial view of the tested plate fins.

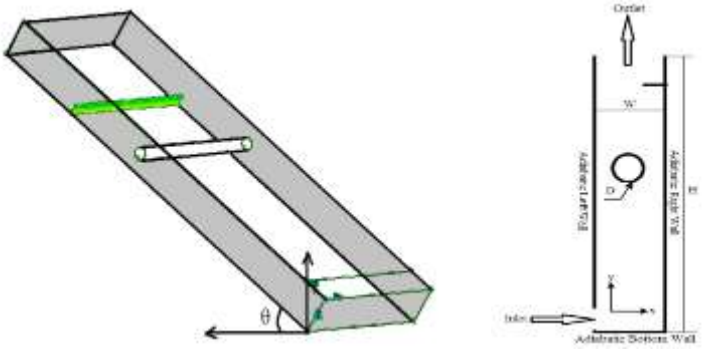

Fig.5: Schematic of problem geometry.

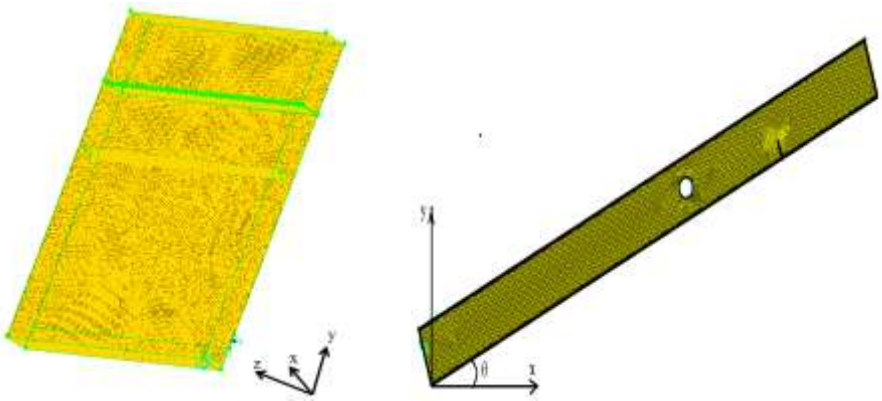

Fig.6: Isometric and Side views of the three dimensional cavity computational domain.

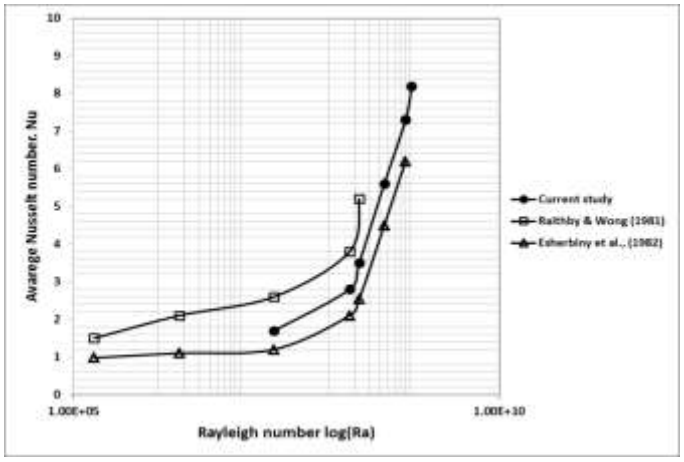

Fig. 7: Validation the present experimental results with previous works.

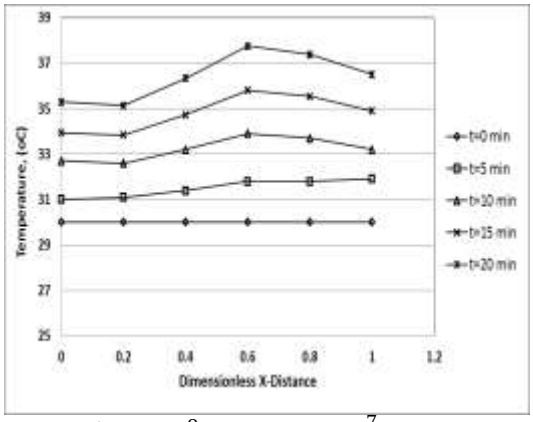

a) θ=90 ^{o}, Ra=3.5 ×10^{7}, s=2 cm

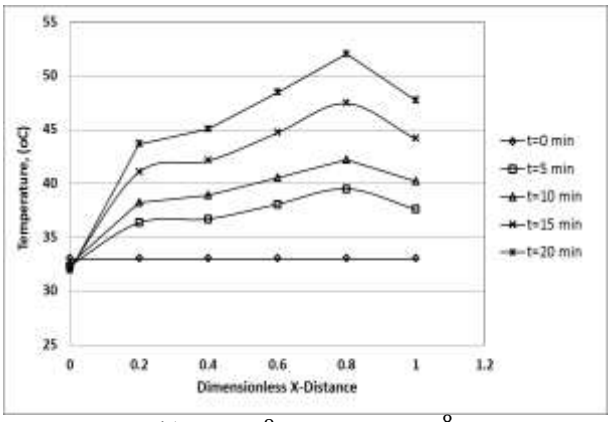

b) θ=90 ^{o}, Ra=4.5 ×10^{8}, s=2cm

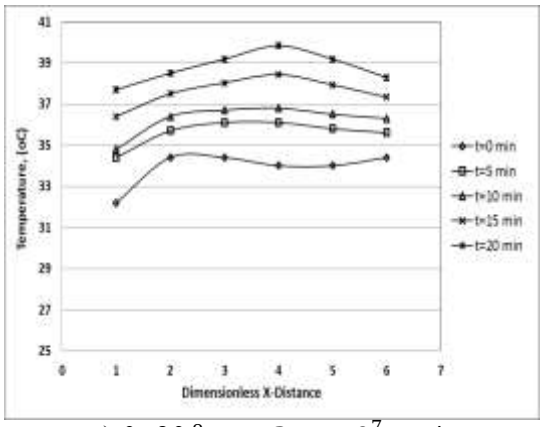

c) θ=90 ^{o}, Ra=3.5 ×10^{7}, s=4 cm

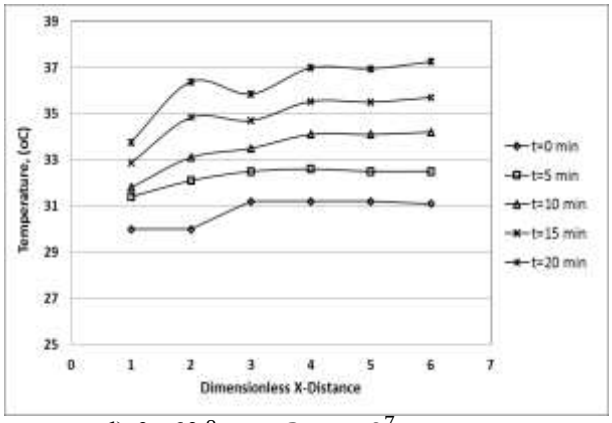

d) θ=60 ^{o}, Ra=3.5 ×10^{7}, s=4 cm

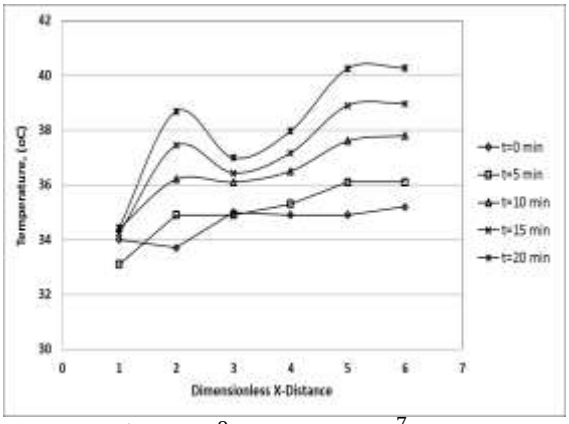

e) θ=30 ^{o}, Ra=3.5 ×10^{7}, s=2 cm

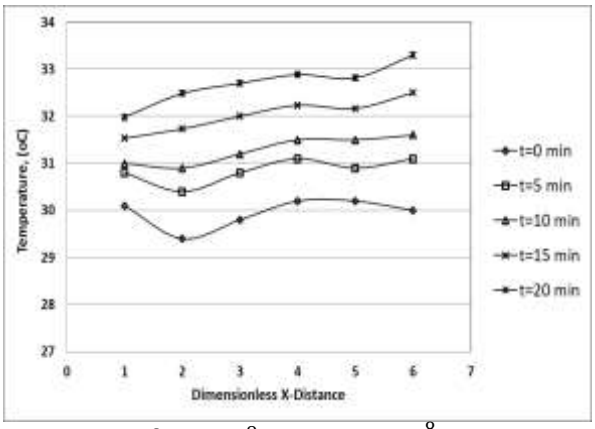

f) θ=30 ^{o}, Ra=4.5 ×10^{8}, s=4 cm

Fig.8: Experimental temperatures distribution along the distance between two vertical walls for smooth fin plates.

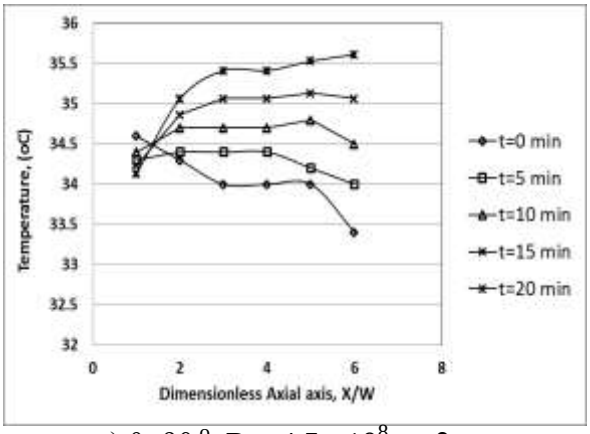

a) θ=90 °, Ra=4.5 ×10^8, s=2 cm

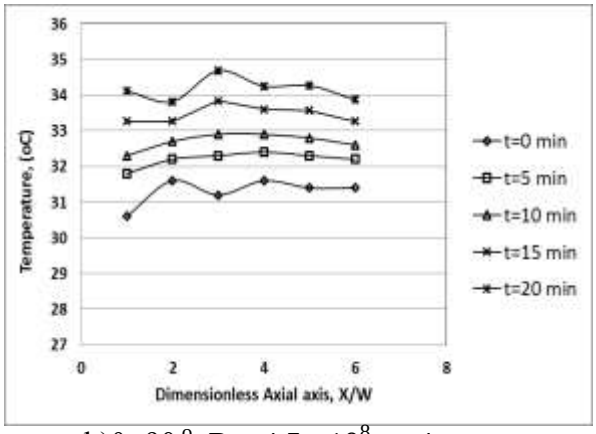

b)θ=90 °, Ra=4.5 ×10^8, s=4 cm

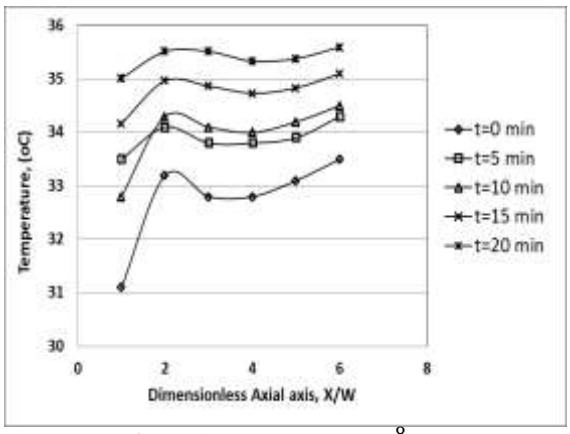

c) θ=60 , Ra=4.5 ×10^8, s=2 cm

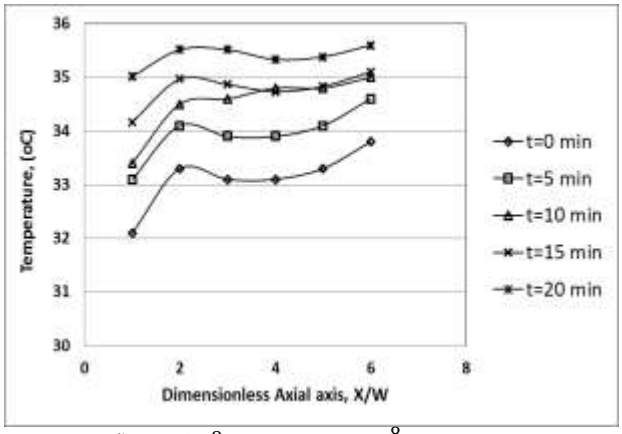

d) θ=60 °, Ra=4.5 ×10^8, s=4cm

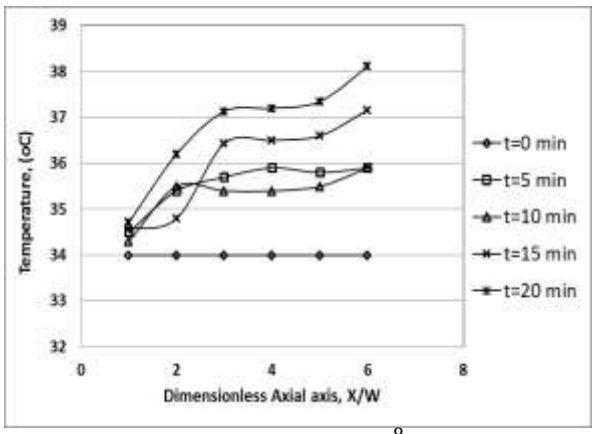

e) θ=60 , Ra=8.3 ×10^8, s=4 cm

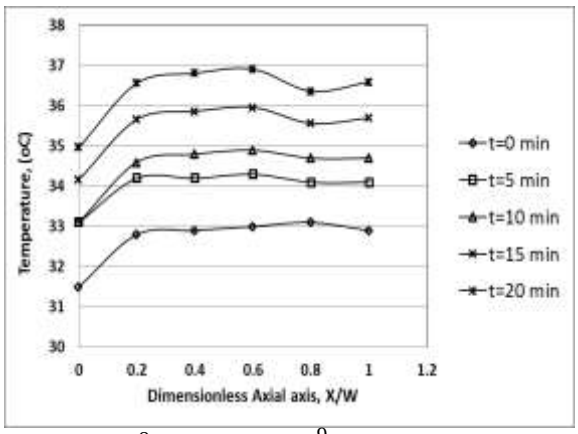

f) θ=60 °, Ra=4.5 ×10^9, s=4cm

Fig.9: Experimental temperatures distribution along the distance between two vertical walls for triangular fin plates.

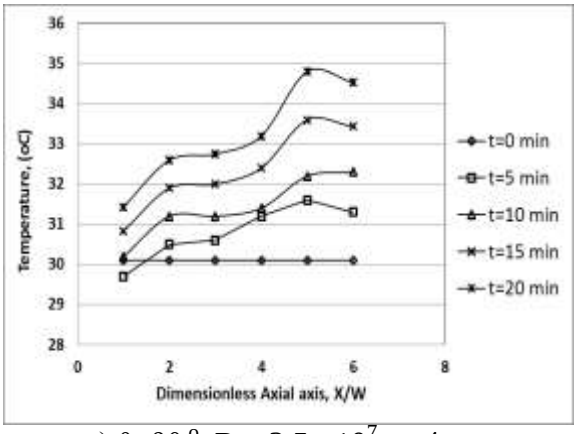

a) θ=90 °, Ra=3.5 ×10^7, s=4 cm

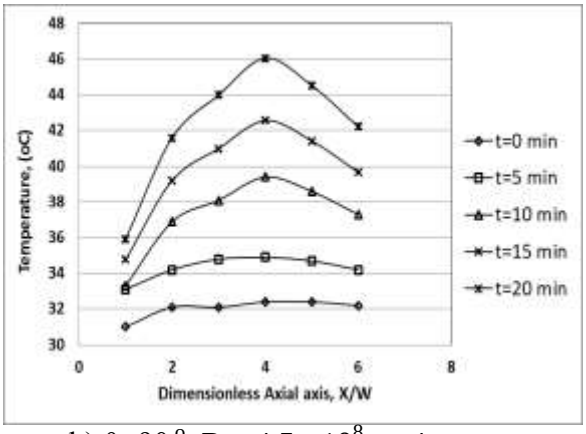

b) θ=90 °, Ra=4.5 ×10^8, s=4 cm

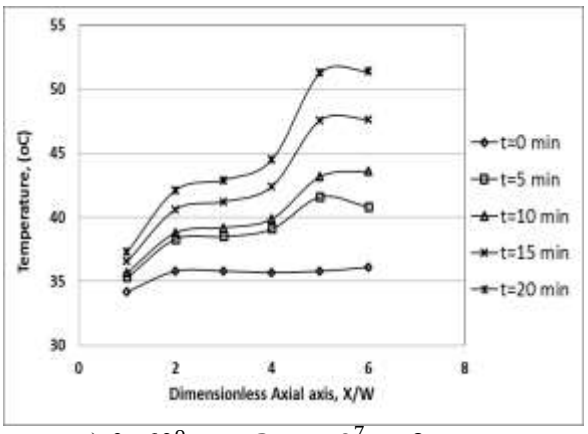

c) θ=60°, Ra=3.5 ×10^7, s=2 cm

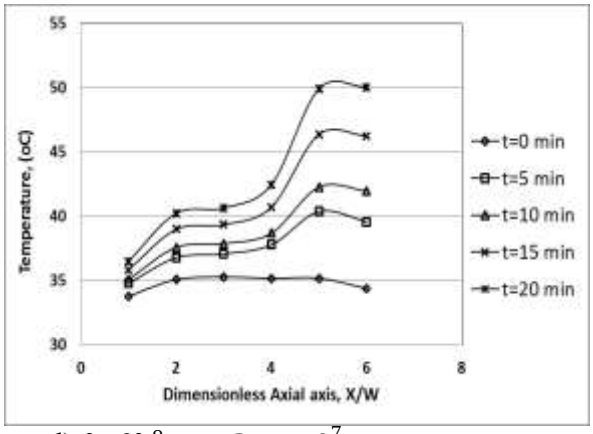

d) θ=60 °, Ra=3.5 ×10^7, s=4 cm

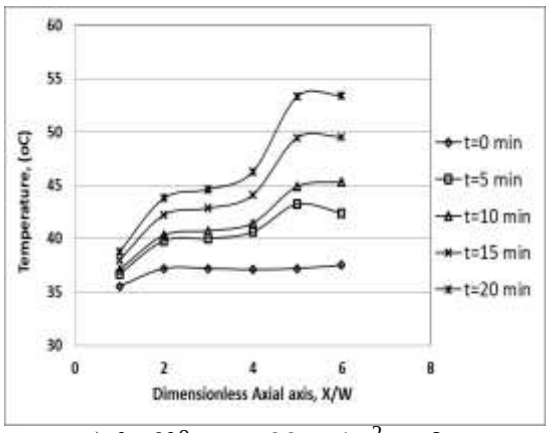

c) θ=60°, q"=500 W/m^2, s=2 cm

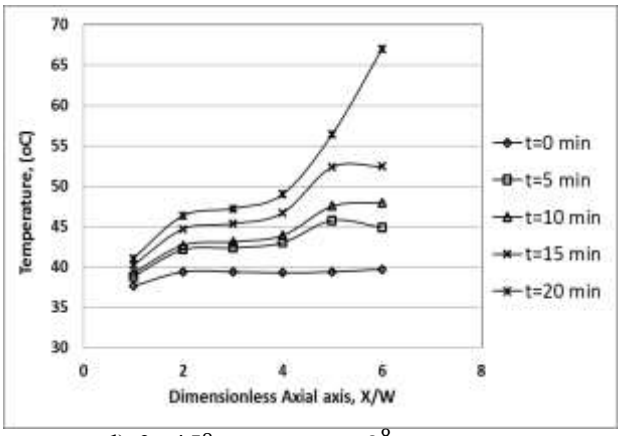

d) θ=45°, Ra=4.5 ×10^8, s=4 cm

Fig.10: Experimental temperatures distribution along the distance between two vertical walls for semi-circle fin plates.

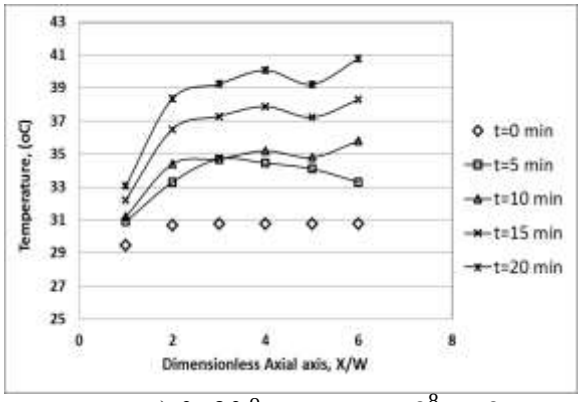

a) θ=90 °, Ra=4.5 ×10^8, s=0 cm

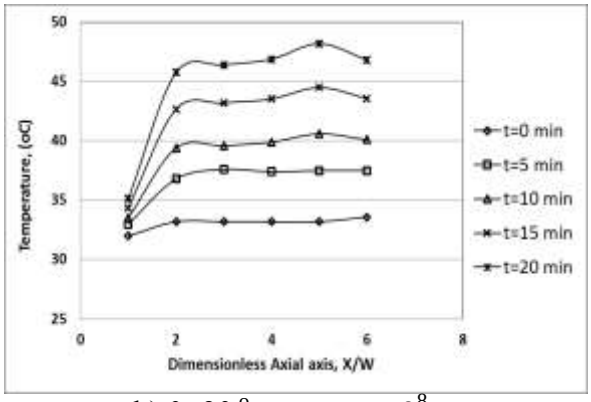

b) θ=90 °, Ra=4.5 ×10^8, s=2 cm

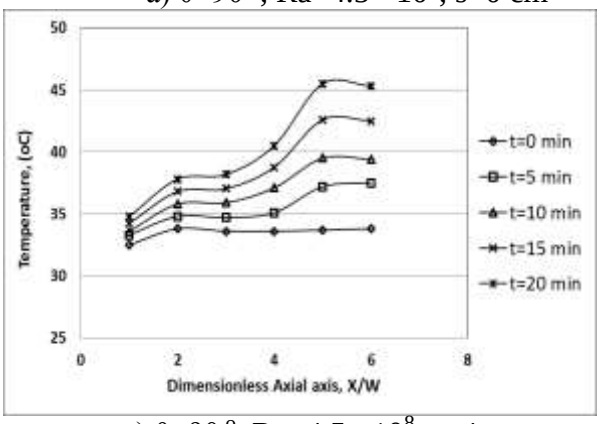

c) θ=90 °, Ra=4.5 ×10^8, s=4 cm

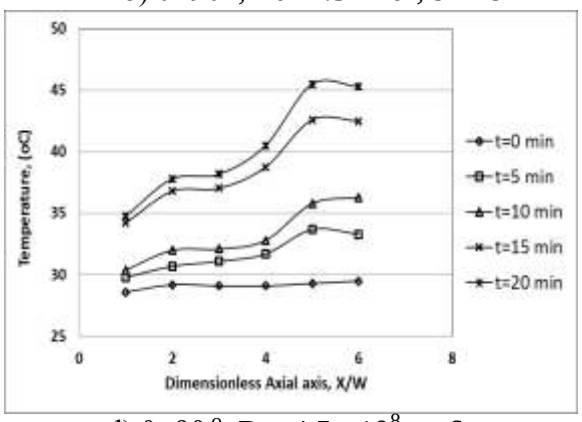

d) θ=90 °, Ra=4.5 ×10^8, s=6 cm

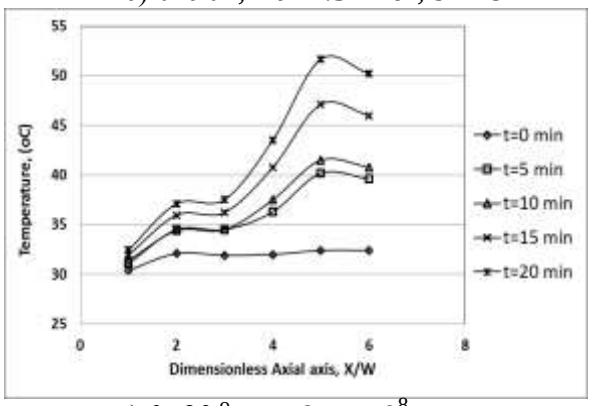

c) θ=90 °, Ra=8.4 ×10^8, s=4 cm

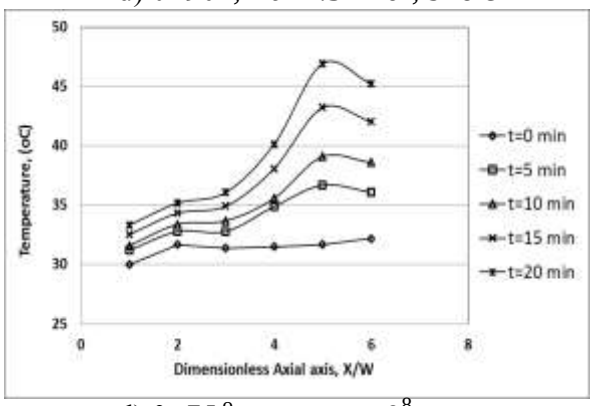

d) θ=75 °, Ra=4.5 ×10^8, s=4 cm

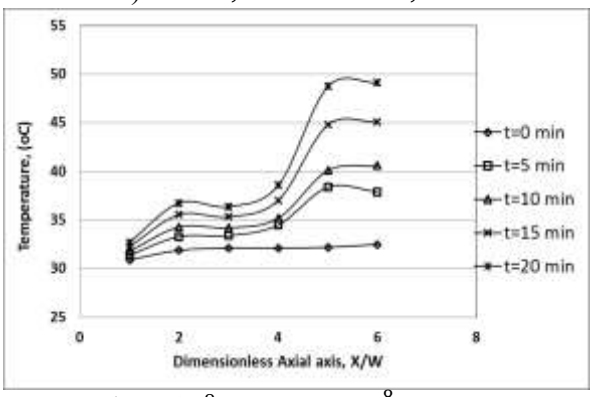

e) θ=60 °, Ra=4.5 ×10^8, s=4 cm

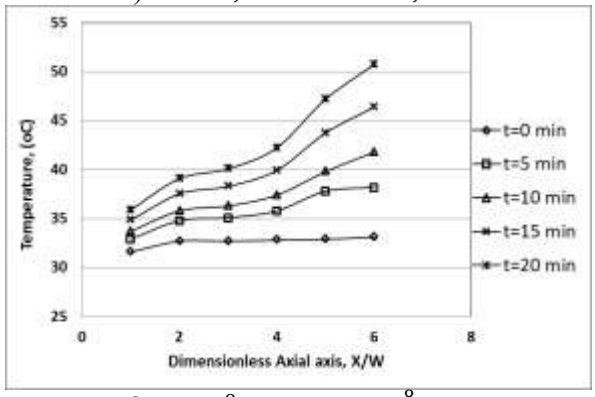

f) θ=45 °, Ra=4.5 ×10^8, s=4 cm

Fig.11: Experimental temperatures distribution along the distance between two vertical walls for square fin plates.

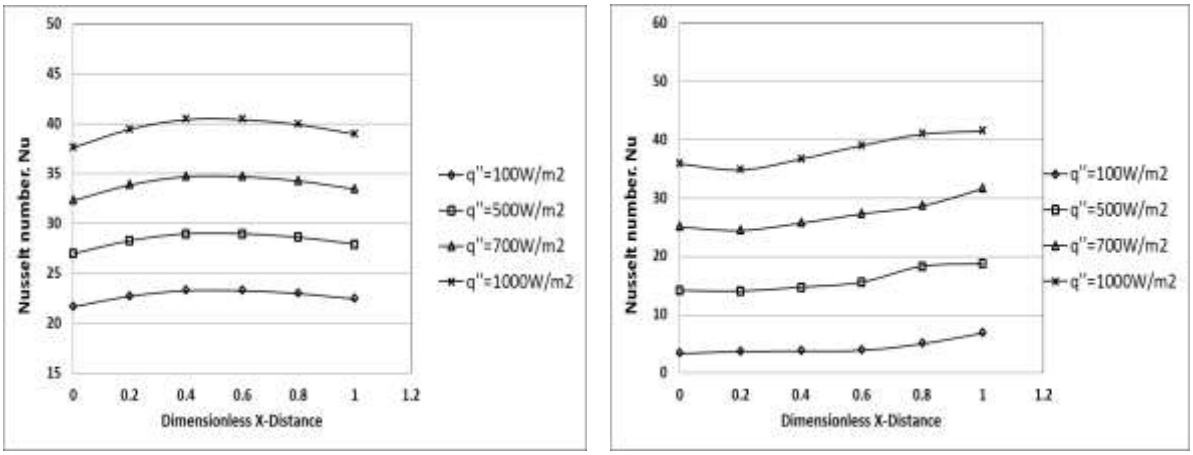

a) Without fin b) Triangular

Fig.12: Experimental Nusselt number (Nu) variation along the distance between two vertical walls for without and triangular fin plates at t=10 min, θ=90^{o}, s=2 cm.

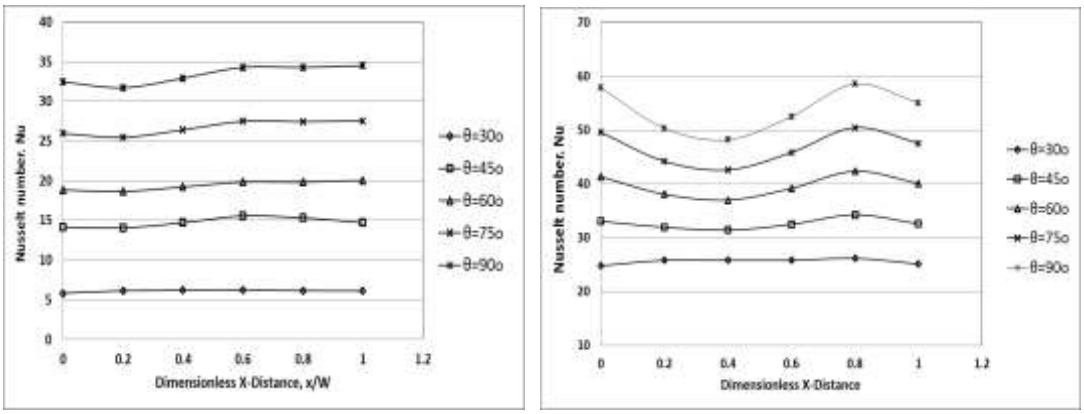

a) Without fin b) Triangular

Fig.13: Experimental Nusselt number (Nu) variation along the distance between two vertical walls for without and triangular fin plates at t=10 min, Ra=4.5 ×10^{8}, s=2 cm.

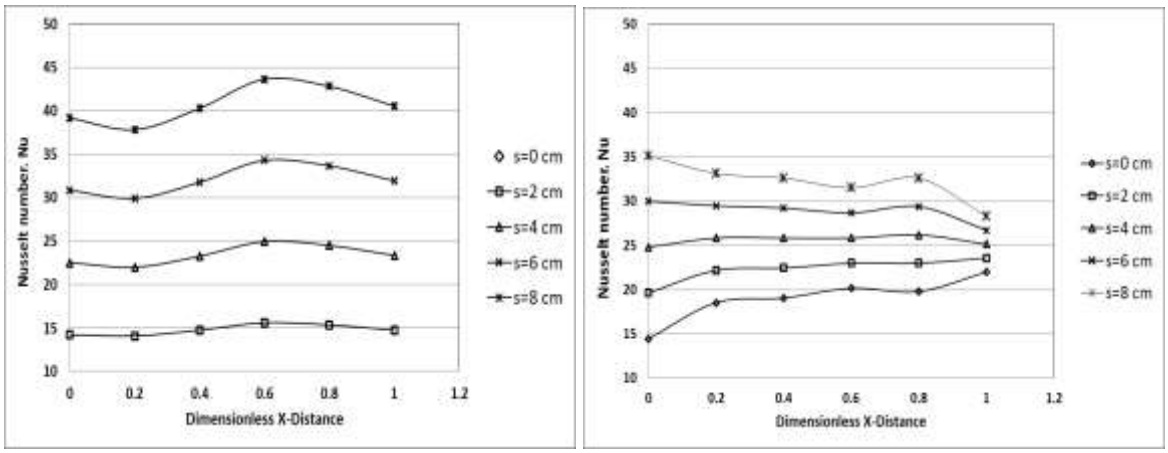

a) Without fin b) Triangular

Fig.14: Experimental Nusselt number (Nu) variation along the distance between two vertical walls for without and triangular fin plates at t=10 min, Ra=4.5 ×10^{8}.

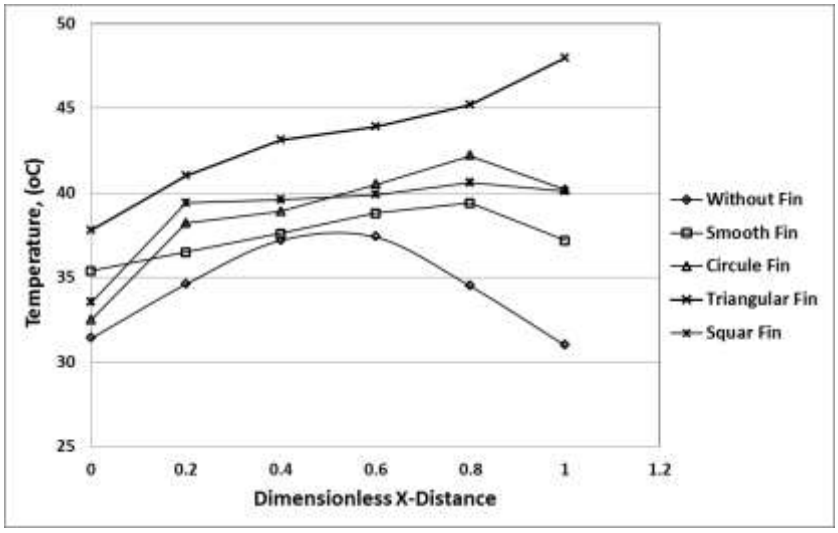

Fig.15: Experimental temperatures distribution along the distance between two vertical walls for all fin plates at t=10 min, Ra=4.5 $\times 10^8$, s=2 cm.

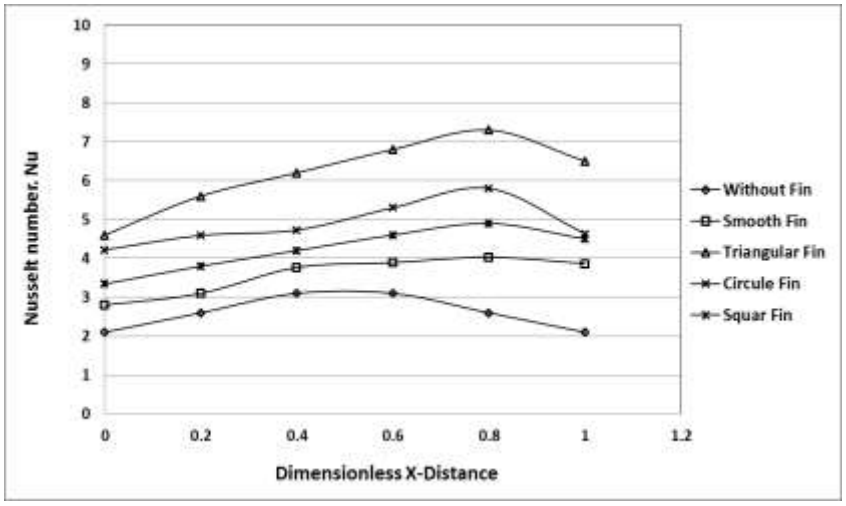

Fig.16: Experimental local Nusselt number (Nu) variation along the distance between two vertical walls at t=10 min, Ra=4.5 $\times 10^8$, s=2 cm.

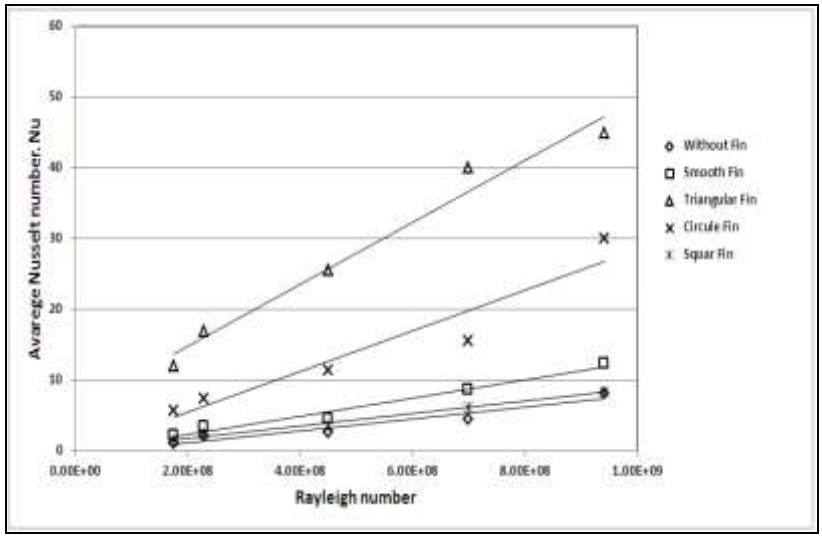

Fig.17: Experimental average Nusselt number (Nu) variation along the distance between two vertical walls plates at θ=90, Ra=4.5 $\times 10^8$, s=2.

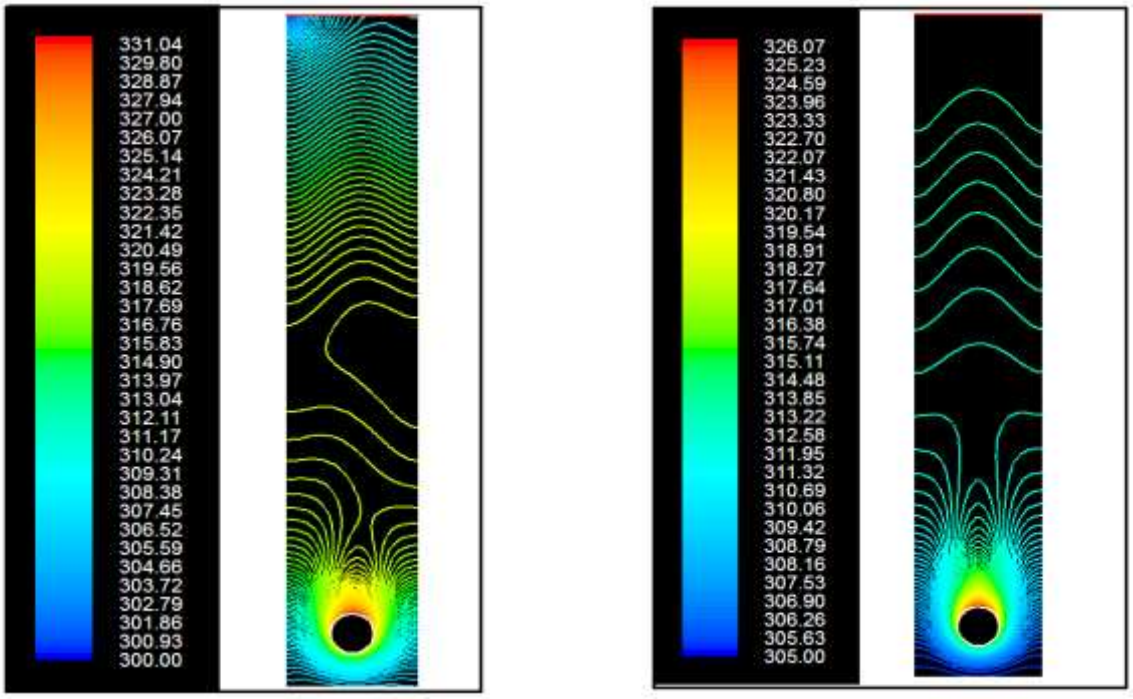

θ=30° θ=90 °

a) Temperatures distribution in (Kelvin).

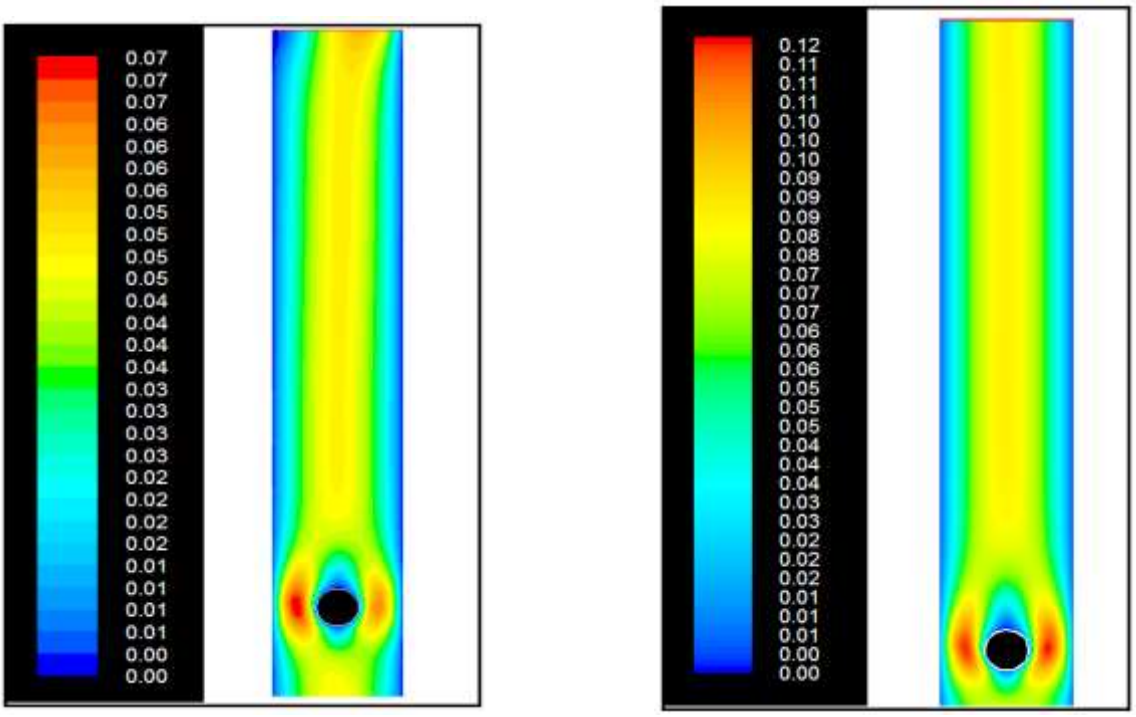

θ=30° θ=90 °

b) Velocity distribution in (m/sec).

Fig.18: Numerical temperatures and velocity distribution between two vertical walls for without fin plate case in the xy-plane at (z=20cm), Ra=4.5 $\times 10^8$, s=4.

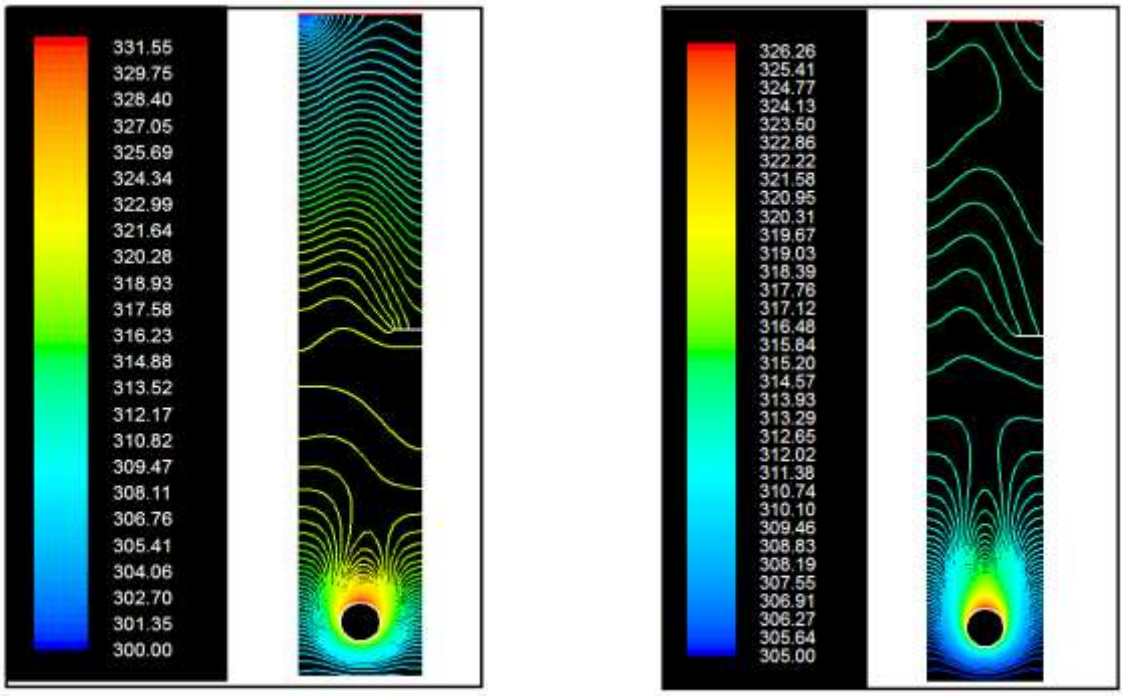

θ=30° θ=90 °

a) Temperatures distribution in (Kelvin).

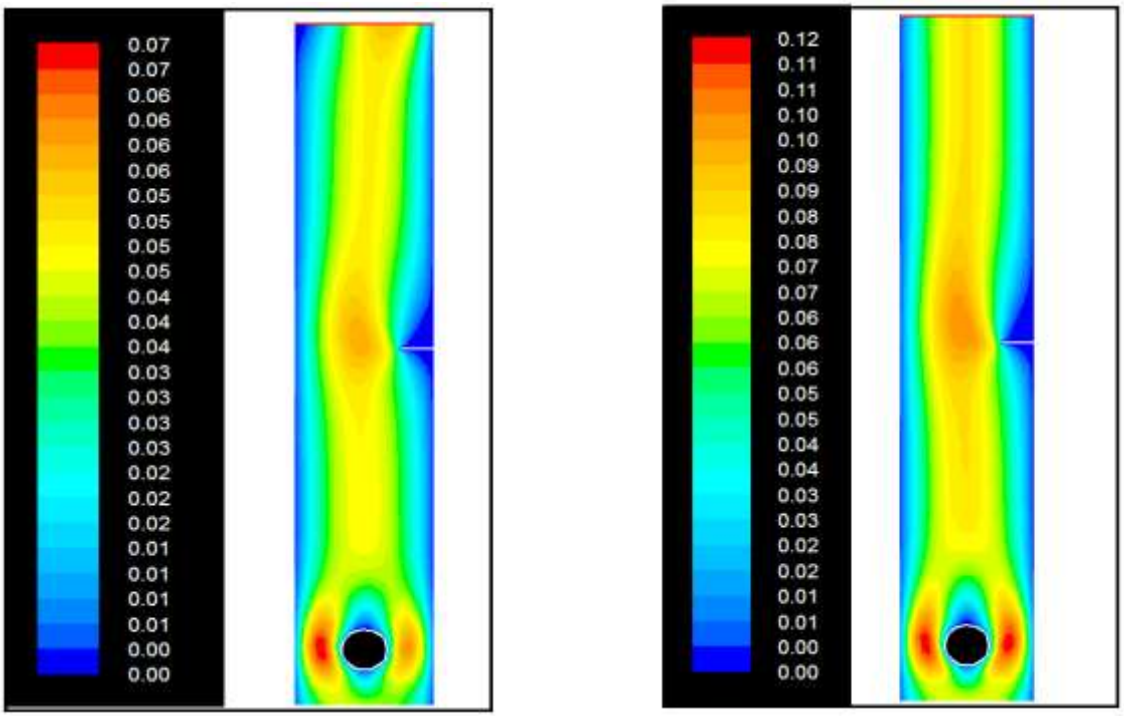

θ=30° θ=90 °

Fig.19: Numerical temperatures and velocity distribution between two vertical walls for smooth fin plate case xy-plane at (z=20cm), Ra=4.5 $\times 10^8$, s=4.

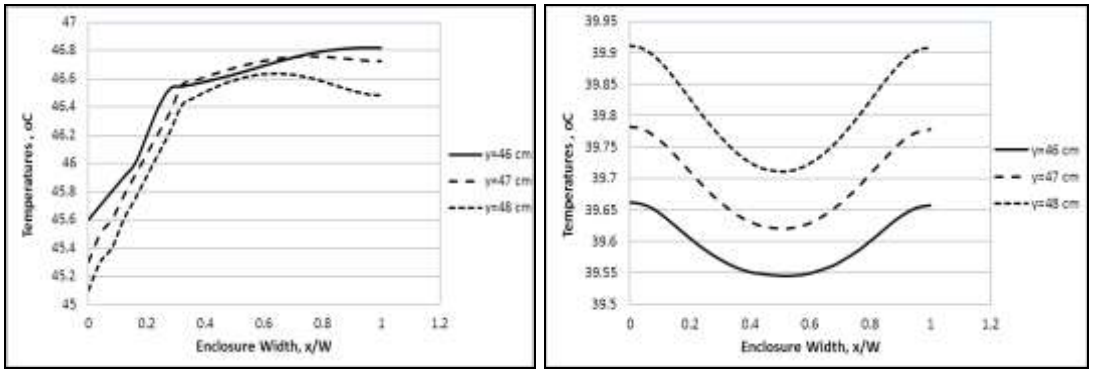

a) Air temperatures

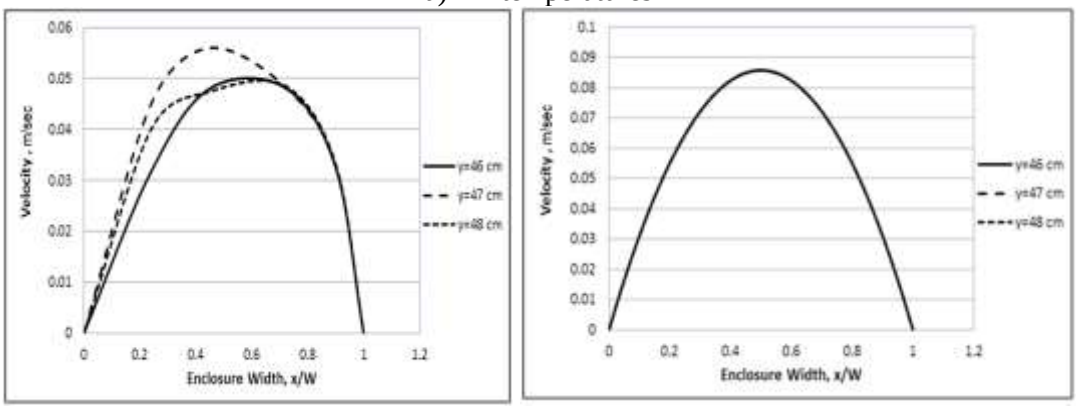

b) Air velocity

θ=30° θ=90°

Fig.20: Numerical temperatures and velocity profile for without fin, just before y=46 cm, in the fin y=47 cm and just after fin y=48 cm; at Ra=4.5 ×10^8, s=4 cm.

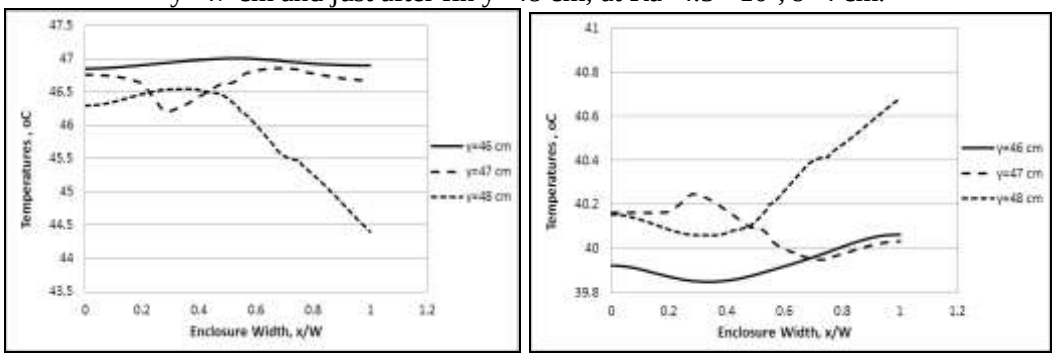

a) Air temperatures

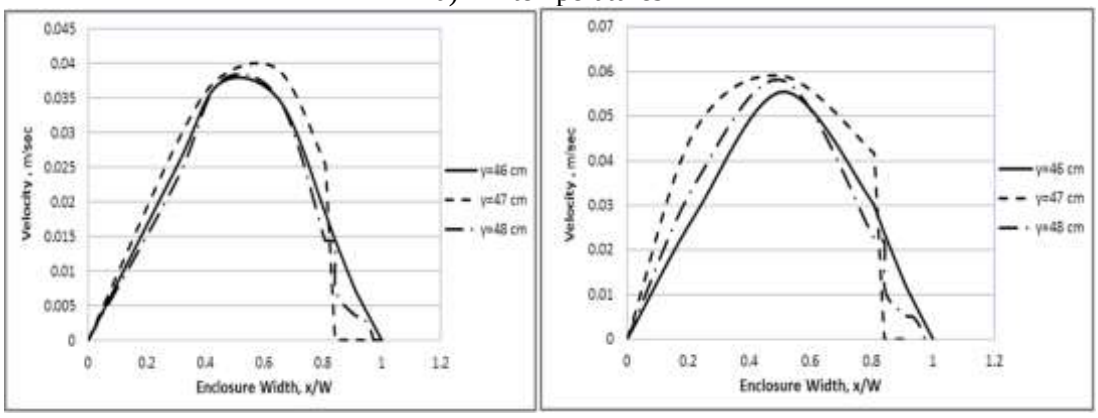

b) Air velocity

θ=30° θ=90°

Fig.21: Numerical temperatures and velocity profile for smooth fin, just before y=46 cm, in the fin y=47 cm and just after fin y=48 cm; at Ra=4.5 ×10^8, s=4 cm.

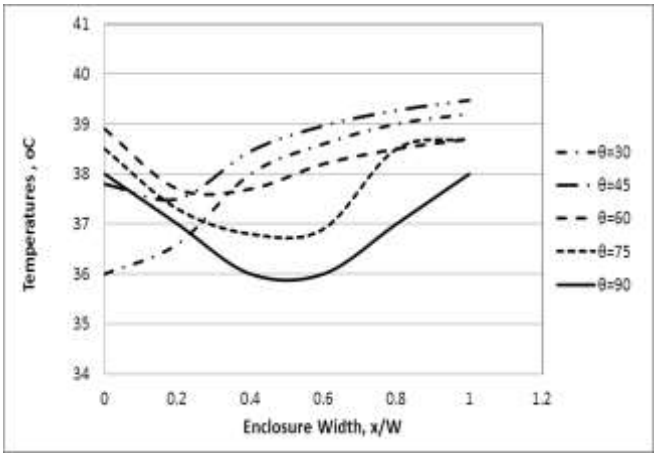

Fig.22: Effect of enclosure title angles on numerical temperatures profile between two vertical walls fin plate case at Ra=4.5 $\times 10^8$, s=4 cm.

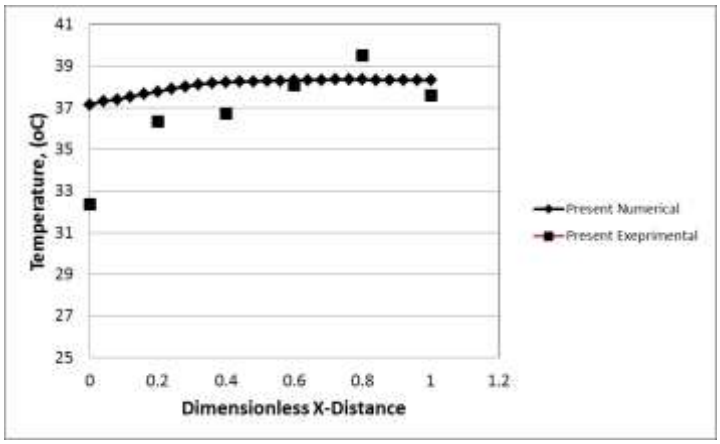

Fig.23: Comparison of the experimental and numerical results for without fins at θ=90^o, (Ra=4.5 $\times 10^8$) , t=10 min, s=4 cm.

Table 1: Uncertainty analysis.

Measurement	Value	Probable error
Outer tube radius (d)	16 cm	± 0.00316 cm
Opening distance (s)	2, 4, 6, 8 cm	± 0.00425 cm
Gap distance (W)	5 cm	± 0.00651 cm
Power voltage (V)	30 volt	± 1.5 volt
Power current (I)	3.5 amp	0.8 amp
Temperature (T)	35 ^{o}C	1.2 ^{o}C

Table 2: Grid independence test results.

Nodes	Outlet temperature (K)	Percentage error (%)
85621	303.2546	2.665
129776	306.4568	1.224
2017421	308.0887	0.826
3075115	308.6256	0.135

Table 3: Presented the applicable correlating present work parameters.

Constants	Without Fin	Smooth Fin	Triangular Fin	Circle Fin
C	0.545	0.225	0.755	0.351
n	0.772	0.879	0.455	0.961
R^2	0.988	0.94	0.9422	0.981

REFERENCES

Abdullatif Ben-Nakhi and Ali J., Chamkha, (2007), Conjugate natural convection in a square enclosure with inclined thin fin of arbitrary length, International Journal of Thermal Sciences 46, pp.467–478.

Ahmed F. Alfahaid (2006), Numerical study of conjugate heat transfer in enclosures with fins attached to vertical side wall, Kuwait J, Sci.33, (2) pp.205-218.

Ahmed F. Alfahaid and R.Y., Sakr, (2005), Numerical Study of Natural Convection Heat Transfer in Enclosures with Conducting Fins Attached to a Vertical Sidewall, 4th International Conference on Heat Transfer, Fluid Mechanics, and Thermodynamics pp.19-22 September, Cairo, Egypt.

ANSYS FLUENT 14.0: Theory Guide, April (2009), ANSYS, Inc. is certified to ISO 9001.

Bilgen, E., (2005), Natural convection in cavities with a thin fin on the hot wall. International Journal of Heat and Mass Transfer 48, pp. 3493–3505.

Davis, G.V., (1983), Natural convection of air in a square cavity, a benchmark numerical solution, Int. J. Numer. Meth. Fluid. 3, pp. 249–264.

Esherbiny, S.M., Raithby, G.D., and Hollands, K.G.T., (1982), Heat Transfer by Natural Convection across Vertical and Incline Air Layers, Transactions of the ASME, vol. 104, pp.96-102.

Fariborz K., Hongtao X., Zhiyun W., M. Yang, and Yuwen Z., (2016), Numerical Simulation of Steady Mixed Convection Around Two Heated Circular Cylinders in a Square Enclosure, Heat Transfer Engineering, 37, (1): pp. 64–75.

Gebhart, B., Y. Jaluria, R. L. Mahajan, and B. Sammakia, (1988), Buoyancy-Induced Flows and Transport. New York: Hemisphere Publishing Corporation.

Holman, J. P., (2012), experimental methods for engineers, eight edition, Department of Mechanical Engineering Southern Methodist University.

Jani S., M. Mahmoodi, M. Amini, (2012), Natural Convection at Different Prandtl Numbers in Rectangular Cavities with a Fin on the Cold Wall, The Journal of Energy: Engineering & Management Vol. 2, No. 4, pp. 58-69.

Kuehn T. H., and R. J. Goldstein, (1980), Numerical Solution to the Navier-Stokes Equations for Laminar Natural Convection About a Horizontal Isothermal Circular Cylinder," International Journal of Heat and Mass Transfer, vol. 23, pp. 971-979.

Lakhal, E. K. , M. Hasnaoui, E. Bilgen, P. Vasseur, (1997), Natural convection in inclined rectangular enclosures with perfectly conducting fins attached on the heated wall, Heat and Mass Transfer 32, pp. 365 – 373.

Launder, B. E., and D. B. Spalding, (1972), Lectures in Mathematical Models of Turbulence. Academic Press, London, England.

McAdams, W. H., (1954), Heat Transmission, 3rd ed. New York: McGraw-Hill Book Company, Inc.

Morgan, V. T., (1975), The Overall Convective Heat Transfer from Smooth Circular Cylinders," Advances in Heat Transfer, vol. 11, pp. 199-264.

Nada, S.A., (2007), Natural convection heat transfer in horizontal and vertical closed narrow enclosures with heated rectangular finned base plate, International Journal of Heat and Mass Transfer 50, pp. 667–679.

Olivier Reymond, Darina B. Murray, Tadhg S. O'Donovan, (2008), Natural convection heat transfer from two horizontal cylinders, Experimental Thermal and Fluid Science 32, pp. 1702–1709

Petr Svarc and Vaclav Dvorak, (2013), Numerical and Experimental Studies of Laminar Natural Convection on A Horizontal Cylinder, engineering Mechanics, Vol. 20, No. 3/4, pp. 177–186.

Pletcher, R. H., J. C. Tannehill, and D. A. Anderson, (2012), Computational Fluid Mechanics and Heat Transfer, 3rd ed. Hoboken, NJ: Taylor and Francis.

Rahman, M. M., Hakan F. Oztop, S. Mekhilef, R. Saidur, A. Ahsan, and Khaled Al-Salem, (2014), Modeling of Unsteady Natural convection for Double-Tube IN A Partially Cooled Enclosure, Numerical Heat Transfer, Part A, 66: pp. 582–603.

Raithby, G.D. and Wong, H.H., (1981), Heat Transfer by Natural Convection across Vertical Air Layers, Numerical Heat Transfer, vol.4, pp.447-457.

Renato José Pinto, Paulo Mohallem Guimarães, Genésio José Menon, (2016), Numerical Study of Natural Convection in Square Cavity with Inner Bodies Using Finite Element Method, Open Journal of Fluid Dynamics, 6, pp. 75-87.

Roslan, R., H. Saleh, I. Hashim, A.S. Bataineh, (2014), Natural convection in an enclosure containing a sinusoidally heated cylindrical source, International J. of Heat and Mass Transfer 70, pp.119-127.

Simon N., Abhimanyu K, Sooraj P.T, Shivanshu C., Vinayak M., (2015), Experimental Insight to the Natural Convection Heat Transfer Transportation Through Perforated Exits, International Journal of Mechanical And Production Engineering, Volume- 3, Issue-8 pp.23-33.